JOURNAL OF SPACECRAFT AND ROCKETS
Vol. 40, No. 2, March–April 2003

Computational Design Approach to Propellant Settling

G. D. Grayson*
The Boeing Company, Huntington Beach, California 92647

A computational approach is devised for the design of propellant-settling systems in rockets and spacecraft for engine restart in low gravity. With a worst-case design approach, 12 numerical experiments are conducted simulating the liquid slosh dynamics during various mission scenarios of an orbital space-maneuvering vehicle that uses a hydrogen peroxide liquid oxidizer and JP-8 liquid fuel. The results indicate that both the liquid kinetic energy and center-of-gravity histories exhibit characteristic shapes that become asymptotic with time. Analysis of these parameters along with visual measurement of slosh wave magnitudes are used to determine the thruster burn times required to settle propellant adequately over the tank outlet. For the vehicle and tank studied, the settling time is a function of tank fill level and varies from 65 to 85 s.

Nomenclature

A_C = vehicle cross-sectional area, ft^2
A_F = antivortex device baffle flow area, ft^2
A_T = antivortex device total baffle area, ft^2
a = ellipsoid maximum x magnitude, ft
a_D = drag acceleration, ft/s^2
a_S = settling acceleration, ft/s^2
Bo = Bond number
b = ellipsoid maximum y magnitude, ft
C_D = antivortex device discharge coefficient
C_D^* = vehicle drag coefficient
c = ellipsoid maximum z magnitude, ft
f = tank fill fraction
h = vehicle altitude, ft
M = vehicle mass, slug
R_T = tank characteristic radius, ft
r_E = Earth's radius, ft
t_{burn} = settling thruster firing time, s
V = antivortex device approach velocity, ft/s
V_{orb} = vehicle orbital velocity, ft/s
x = x-direction coordinate, ft
y = y-direction coordinate, ft
z = z-direction coordinate, ft
ΔP = antivortex device baffle pressure loss, lbf/ft^2
θ = initial free-surface angle, deg
μ_E = Earth's gravitational constant, ft^3/s^2
μ_L = liquid viscosity, slug/ft · s
ρ_A = atmospheric density, slug/ft^3
ρ_L = liquid density, slug/ft^3
σ_L = liquid surface tension, lbf/ft

Introduction

IN low-gravity environments such as Earth orbit, liquid location inside of storage tanks is influenced not only by acceleration but also by tank geometry and significant surface-tension forces. For launch vehicles and spacecraft containing liquid propellants, the fuel and oxidizer can move away from their respective tank outlets and, thus, permit the flow of both liquid and gas phases into the propellant feed system. Ingestion of gas into a liquid propellant engine can cause failed ignition, premature shutdown, thrust fluctuations, damage to turbomachinery, or catastrophic failure. To guarantee a bubble-free liquid propellant supply, the tank outlet must be submerged in liquid during engine operation. For tanks that do not have propellant management devices, which hold liquid over the outlet or acquire propellant with liquid-acquisition channels or vanes, a propellant settling maneuver can be performed to submerge the tank sumps in preparation for an engine start in orbit. Typically, this is performed by firing separate aft-facing thrusters on the vehicle to yield a positive axial acceleration environment that moves the vehicle toward the liquid. For a given vehicle and engine-firing scenario, the time required to settle propellants must be determined in advance so that the thruster operation logic can be incorporated into the vehicle software. The approach detailed here is a systematic means of determining not only adequate thruster firing times but also the sensitivity of propellant-settling performance to vehicle parameters. This provides a thorough characterization of the relevant fluid physics, which can then be used by propulsion system designers to improve design robustness in multiple mission environments and to minimize the setting propellant use on orbit.

Presented as Paper 2000-5151 at the AIAA Space 2000 Conference, Long Beach, CA, 19–21 September 2000; received 29 May 2001; revision received 6 November 2002; accepted for publication 6 November 2002.

*Principal Engineer/Scientist, Phantom Works, Mail Stop H013-C313. Senior Member AIAA.

Approach

A series of 12 computational fluid-dynamic simulations using the FLOW-3D[1] software are performed to determine the required thruster firing times that ensure adequate propellant settling during all mission scenarios. This is performed for a candidate space maneuvering vehicle that uses hydrogen peroxide (H_2O_2) and JP-8 for propellants; however, the methods presented are readily applicable to any space propulsion system that uses settling as a means of liquid acquisition. Only the H_2O_2 tank is modeled in the present study. Because of its much larger size and, hence, much larger kinetic energy during settling, settling times will be longer for the oxidizer tank than for the smaller JP-8 fuel tank. Accordingly, if the H_2O_2 tank is adequately settled, then the JP-8 tank is also settled. Refer to the block diagram in Fig. 1 for a summary of the comprehensive approach to propellant-settling design that is explained thereafter.

Orbital Drag

Before a simulation is executed, some worst-case assumptions are determined. The orbital drag acceleration serves to position the propellant in a specific location within the tank. For a vehicle flying nose first, the propellant tends to settle against the forward tank dome or opposite an aft-located tank outlet. Using Newton's second law and a drag force proportional to dynamic pressure, the orbital drag acceleration on the spacecraft can be estimated as

$$a_D = C_D^* A_C \rho_A V_{\text{orb}}^2 \big/ 2M \tag{1}$$

where C_D^* is an effective drag coefficient relevant in a rarified fluid, A_C is the vehicle cross-sectional area facing the direction of motion, and ρ_A is atmospheric density at a given altitude. Orbital velocity is determined via the classical relationship

$$V_{\text{orb}} = \sqrt{\mu_E/(r_E + h)} \tag{2}$$

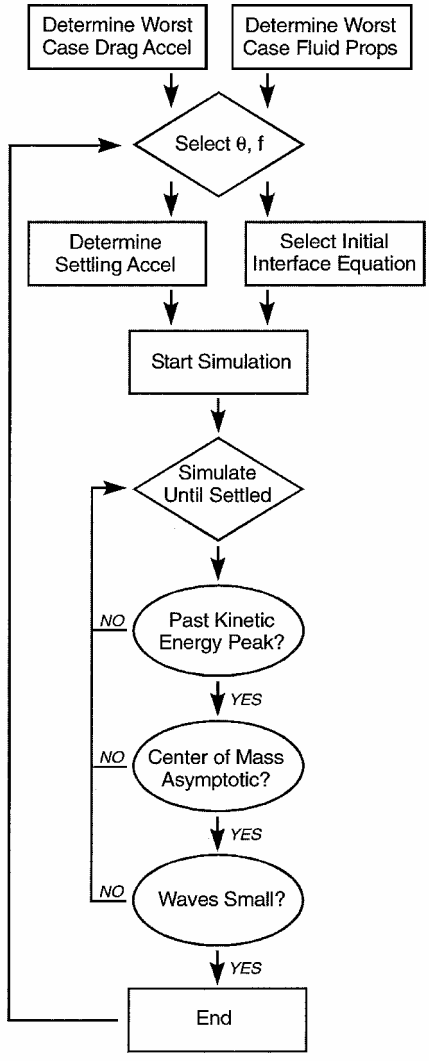

Fig. 1 Approach block diagram.

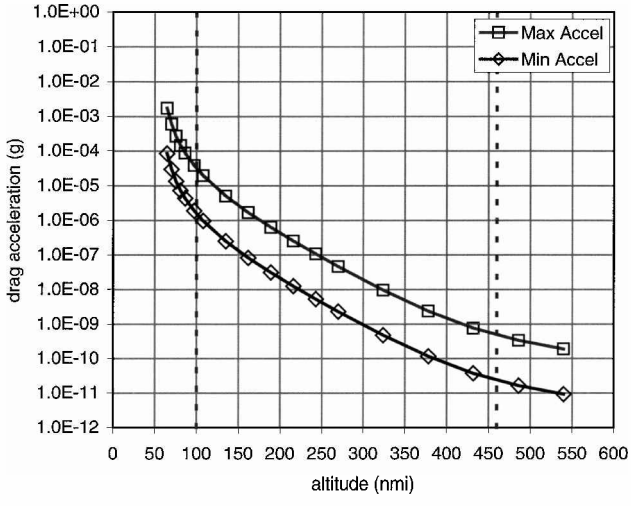

Fig. 2 Orbital drag vs altitude.

C_D^* is estimated to be 2, and the cross-sectional area varies from 36 to 333 ft^2. The assumed vehicle mass is between 6000 and 13,200 lbm. Based on the provided inputs and environmental constants, the orbital drag is calculated as a function of altitude, as illustrated in Fig. 2.

In Fig. 2, the vertical dashed lines indicate the spacecraft altitude range, whereas the two curves shown illustrate minimum and maximum drag acceleration levels based on the vehicle cross-sectional area range. The maximum predicated drag within the vehicle's altitude range is $3.85E-5$ g. Because higher accelerations can position the bulk propellant farther from the tank outlet due to less wetting of internal surfaces, this maximum drag is used in all calculations in the present study. It is assumed that the liquid–gas interface is in equilibrium at the start of each simulation and, hence, quiescent. The drag acceleration computed is used to estimate the initial equilibrium interface shape as will be described.

Fluid Properties

A further worst-case measure involves the selection of liquid properties. The H_2O_2 in the tank is maintained above 1 atm in pressure and between 37 and 120°F in temperature. Under these conditions, hydrogen peroxide is considered an incompressible fluid; hence, its physical properties are mostly a function of temperature. During the relatively short propellant-settling maneuvers, it is assumed that the bulk liquid temperature does not change significantly. Accordingly, constant liquid properties with no phase change or decomposition are used in all cases. Propellant settling in reduced gravity is a function primarily of 1) buoyancy, 2) inertia, and 3) surface-tension forces. The buoyancy force is the effect of firing the thrusters, inertia involves the resulting motion and fluid impacts, and surface tension is a stabilizing force that serves to maintain a curved liquid–gas interface and, hence, minimum surface energy or free energy.[2] Thus, for propellant settling, the worst-case liquid properties have low density, low viscosity, and low surface tension. The low density reduces the effect of buoyancy due to slightly less density difference between phases, whereas low viscosity and surface tension yield more splashing and longer equilibrium interface transients. Because all three fluid parameters decrease with increasing temperature in the given range, the maximum storage temperature of 120°F and the associated properties are used in all calculations of the present study. Accordingly, the H_2O_2 density ρ_L is 2.6431 slug/ft^3, the viscosity μ_L is $1.7415E-5$ slug/ft · s, and the surface tension σ_L is $5.1216E-3$ lbf/ft. Note that, due to limited surface tension data, σ_L is linearly extrapolated to 120°F from two points (32 and 68°F), and the contact angle between the liquid and tank is assumed to be zero.

Fill Fraction

To characterize the dynamic slosh environment within the tank during settling, six different fill fractions f are investigated. The fill levels selected span the minimum and maximum range during a mission and are 4, 10, 30, 50, 70, and 95.5%. The 4% fill level is selected as the minimum propellant load for a main engine firing. The maximum fill level is 95.5%, which reflects a 4.5% initial ullage volume fraction.

Settling Acceleration

Once a fill level is selected, the mass of the vehicle and the resulting acceleration during settling can be computed. A linear relationship is derived to approximate total vehicle mass as a function of fill fraction. The vehicle is presumed to have a mass of precisely 6000 lbm at a 0% fill fraction and 13,200 lbm at 95.5%. With the assumed 10 lbf thrust during settling used, the acceleration is readily tabulated as shown in Fig. 3.

Thruster Firing Mode

The settling acceleration can be applied continuously or in discrete pulses. In continuous settling, the thrusters are fired nonstop until the propellant is settled. In pulse mode, the thrusters are fired for a short duration and then turned off for some time. This on–off cycle is performed repeatedly until the propellant is settled. In many spacecraft designs use of pulse settling can reduce propellant consumption substantially over a continuous-burn approach.[3,4] Basically, once the propellant is moved to the aft of the tank, it can be maintained there with very low average accelerations. However, in propellant tanks with large baffles or complex propellant management devices, operating the thruster in a pulse mode may not yield enough average acceleration to settle the propellant adequately. This is due to the typically large surface-tension-to-buoyancy force ratios associated with the internal tank hardware. Thus, baffles will tend to trap propellant at the intersections with the tank wall due to the

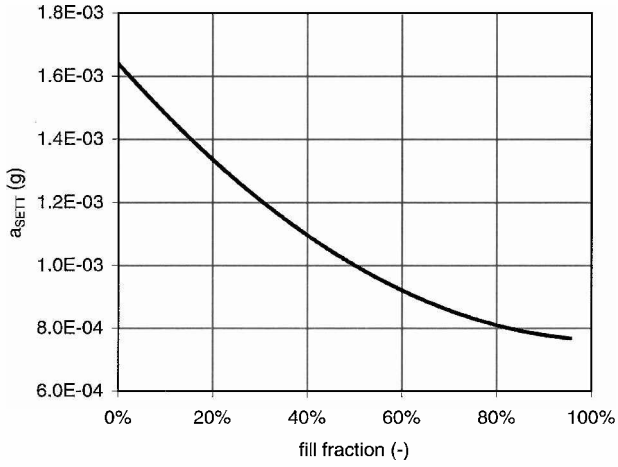

Fig. 3 Settling acceleration vs fill fraction.

locally large surface tension. Here the reduced average acceleration caused by pulsing the thrusters may not be enough to remove the wicked propellant. Additionally, vehicles that have several orbital engine restarts and coast periods are more likely to have dry sumps when settling is initiated. Therefore, any gas in the tank outlet must be flushed out during the settling operation. Because of the tank internal hardware and mission environment continuous settling is selected for the present design problem.

Initial Orientation

The initial liquid orientation is defined as an angle θ measured counterclockwise from the vehicle centerline to the unit normal of a flat or settled free surface. Thus, a value of 0 deg places the propellant against the forward dome, a value of 90 deg is against the side of the tank, and a value of 180 deg is against the aft dome. In the present analysis, two values of θ are used with the six selected fill fractions. The 0-deg condition is sometimes assumed to be the worst in terms of propellant settling because the liquid is initially as far away from the outlet as possible. However, simulations at $\theta = 20$ deg are executed to investigate the circular liquid motion that frequently occurs during settling as the liquid slides down the tank side wall and continues past the outlet due to its inertia. With a symmetric 0-deg initial condition, the propellant kinetic energy can become substantially damped due to colliding slosh waves at the bottom of the tank.

Initial Interface Shape

Two different initial interface shapes are used in the present study: flat and curved. For the $\theta = 20$ deg cases, a flat free surface is assumed for the beginning propellant condition. Although the actual liquid–gas interface tends to be highly curved in low gravity, a flat free surface places the propellant farther away from the outlet, thus, yielding higher kinetic energy and splashing during settling.

A more accurate initial condition is derived for the symmetric $\theta = 0$ deg cases. In low gravity, surface tension forces form a liquid–gas interface shape that balances the tendency toward both minimum surface and potential energies.[2] Therefore, the more surface tension dominates acceleration, the more curvature there is in the liquid–gas interface. Conversely, as acceleration dominates, the liquid–gas interface becomes flatter. A measure of the relative buoyancy and surface-tension forces is the nondimensional Bond number, which is defined as

$$Bo \equiv \rho_L a_S R_T^2 / \sigma_L \tag{3}$$

where a_S is settling acceleration. When the Bond number is significantly less than unity, surface-tension forces dominate, and the radius of curvature of the interface approaches that of the container. For the present problem, the Bond number during the low-gravitational acceleration coast period before settling is 3.4, which indicates that the interface shape is curved and not flat. Because an ellipsoid approximates this shape between a flat surface (high Bond number) and a sphere (low Bond number), the initial free surface for the $\theta = 0$ cases is specified by the classical second-order equation for an ellipsoid:

$$(x - x_0)^2 / a^2 + (y - y_0)^2 / b^2 + (z - z_0)^2 / c^2 = 1 \tag{4}$$

A further simplification applicable only to the $\theta = 0$ deg simulations is that the free surface is also an oblate spheroid with the semiminor axis aligned with the drag acceleration vector, thus an ellipsoid with $a = b$. The initial ellipsoidal aspect ratio is then defined as a/c, which is determined as a function of the presettling acceleration vector. For the calculated maximum orbital drag of $3.85E{-}5\ g$, an interface aspect ratio of 2.5 is selected. This value is based on the interface shape predicted by FLOW-3D under a constant drag acceleration. The resulting free-surface shape is approximate but is more accurate than a spherical or flat free-surface assumption. This method is used for prescribing all $\theta = 0$-deg initial liquid–gas interfaces.

FLOW-3D Simulations

The FLOW-3D computational fluid-dynamics software is a general Navier–Stokes equation solver, well established in liquid slosh problems.[1] The software is proven to be accurate for both large-amplitude slosh problems[5] and sloshing liquids in very large containers.[6] Verification of the software as an aerospace design tool is achieved via flight testing, where a successful in-atmosphere propellant-acquisition system is designed by simulation only, with no testing.[7] In low-gravity, surface-tension-dominated environments, FLOW-3D is validated via drop tower[8] and parabolic-trajectory aircraft experiments.[9] FLOW-3D's aerospace history and relevant code validation make it an excellent software tool for the present propellant-settling problem.

Tank Model

The 4.6-ft-diam, 5.6-ft-long oxidizer tank is discretized by 529,200 computational hexahedral cells, which adequately resolve all pertinent tank geometric features (Fig. 4). All surfaces are specified with second-order polynomial equations and include the internal tank wall surface, three 3.75-in.-wide annular slosh baffles, sump, and antivortex baffles.

All three slosh baffles in the model are resolved by one numerical cell and are 1 in. thick. The modeled thicknesses are larger than in an actual vehicle, but this reduces the computational resource requirements for each simulation. The calculation results are not significantly affected by this artificial fattening of the baffles because the tank is several orders of magnitude larger. The width of each baffle is resolved by five cells, which is adequate to model the bulk slosh.

The antivortex device is cruciform shaped and constructed of perforated baffle plates 5 in. tall, 12 in. wide, and 27% porous.

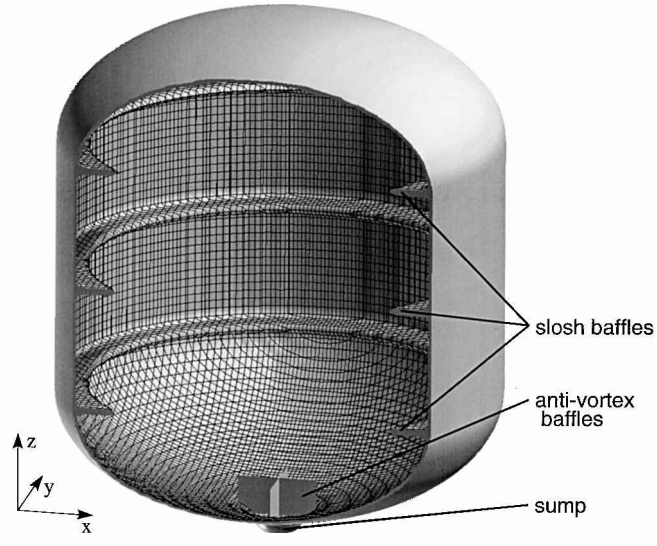

Fig. 4 H_2O_2 tank model.

It is modeled with infinitely thin planar surfaces resolved by a 20×9 mesh. A velocity-squared pressure-loss relationship is employed across the baffle plates according to the following equation[10]:

$$\Delta P = 1/C_D^2\left[(A_T/A_F)^2 - 1\right]\left(\rho_L V^2/2\right) \tag{5}$$

where ρ is H_2O_2 density. The discharge coefficient is 0.72 and is determined based on previous test data for flow through perforated plates.[10,11]

Model Assumptions

Several simplifying physical assumptions are made in the FLOW-3D model: 1) laminar flow, 2) no wall shear, 3) constant liquid properties (ρ_L, μ_L, σ_L), 4) isothermal, 5) no phase change or decomposition, 6) antivortex baffle pressure loss proportional to velocity squared, 7) 1-in.-thick baffles with no vent holes, 8) ellipsoidal or flat initial interface shapes, and 9) 1 s of drag acceleration before settling.

Low-gravity settling flows are generally laminar due to the low velocities imparted to the liquid by small ($\ll 1$ g) settling accelerations. When wall shear is neglected, the boundary layers are assumed to be infinitely thin, which is justifiable for bulk slosh in large tanks. Furthermore, the enforcement of no slip at the tank surfaces would yield a less conservative solution due to the additional viscous damping. The liquid properties are all constant and isothermal with no phase change or decomposition as already discussed. Use of thicker baffles has little effect on the bulk liquid motion due to the much larger size of the tank; similarly, the omission of vents in the baffle are neglected because the vent flow area is much smaller than the total baffle area. An ellipsoidal liquid–gas interface is used in the $\theta = 0$-deg cases, whereas a flat interface is employed in the $\theta = 20$-deg cases as discussed earlier. At the start of each calculation, the liquid is subjected to 1 s in the low-gravity drag field. This initial period under a constant low-gravity drag field reduces some of the bubble recoil due to a nonexact initial interface specification.

Model Operation

Each simulation is initiated once the initial interface is specified and the acceleration history is determined. After 1 s of drag, the acceleration is increased to the specified settling level over a 10-ms linear ramp. The acceleration is applied continuously until the propellant is settled, after which the calculation is stopped. The FLOW-3D results are then postprocessed to yield time histories for liquid center of mass and mean kinetic energy. Three-dimensional graphic data are also output for each case from which tank outlet coverage and slosh wave sizes are directly observed. Table 1 shows the numerical test matrix, where the case number, initial propellant angle, fill fraction, vehicle mass, drag acceleration, settling acceleration, and initial interface shape are shown.

Propellant-Settling Criteria

Historically, determining when propellant is adequately settled for engine start has been somewhat subjective and based either on film analysis of experiments or computational fluid-dynamic graphics. Some attempts have been made to quantify settling by nondimensional numbers,[12] but this has been for unbaffled tanks and is not directly applicable for tanks with baffles. In the present work, a method is used to evaluate settling that utilizes measurable parameter histories and simulation graphics.

Table 1 FLOW-3D simulation test matrix

Case	θ, deg	f, %	M, lbm	a_D, g	a_S, g	Interface
1	0	4	6,314	$3.85E-5$	$1.58E-3$	Ellipsoid
2	0	10	6,785	$3.85E-5$	$1.47E-3$	Ellipsoid
3	0	30	8,356	$3.85E-5$	$1.20E-3$	Ellipsoid
4	0	50	9,927	$3.85E-5$	$1.01E-3$	Ellipsoid
5	0	70	11,500	$3.85E-5$	$8.70E-4$	Ellipsoid
6	0	95.5	13,200	$3.85E-5$	$7.58E-4$	Ellipsoid
7	20	4	6,314	$3.85E-5$	$1.58E-3$	Flat
8	20	10	6,785	$3.85E-5$	$1.47E-3$	Flat
9	20	30	8,356	$3.85E-5$	$1.20E-3$	Flat
10	20	50	9,927	$3.85E-5$	$1.01E-3$	Flat
11	20	70	11,500	$3.85E-5$	$8.70E-4$	Flat
12	20	95.5	13,200	$3.85E-5$	$7.58E-4$	Flat

A distinction is made between the liquid dynamics in unbaffled and baffled propellant tanks in low gravity. An unbaffled tank, or one with smooth walls and no slosh baffles, typically exhibits a geyser flow following the first impact of propellant on the aft tank surface. The liquid flows mostly down the tank side walls, impacts near the tank drain, and then traverses, or geysers, back upward to the forward end of the tank. After a series of geysers, the propellant damps and becomes settled. This geysering behavior has been observed on previous rocket stages[13] and in parabolic aircraft experiments.[15] Several software models have been able to represent adequately the geysering in unbaffled tanks.[3,4,9,12,14,15] In propellant tanks containing one or more baffles that are typically annular in shape, the geysering problem is much less pronounced due to the dynamic damping and wave interaction that occurs as liquid flows around and impacts on the baffles. Once the bulk liquid reaches the aft section of the tank, any upward motion along the walls is deflected and damped, thus, decreasing the liquid's kinetic energy. The inverse is true as well in that the baffles restrict flow aftward toward the outlet.

In the present analysis, a method is defined to characterize propellant settling for tanks with and without baffles. Independent of flow obstructions within propellant tanks, the liquid mean kinetic energies and center-of-mass histories exhibit characteristic shapes common to all settling scenarios. The mean kinetic energy is a direct measurement of velocity in the liquid. For a given propellant-settling scenario, the liquid initially has some small kinetic energy, increases to a peak value, then decreases as the liquid motion is damped. This described kinetic energy history is typical of all settling problems, although some may oscillate following the peak value and some may not be as pronounced as others.

The center-of-mass (or c.g.) histories also demonstrate an asymptotic behavior where the c.g. starts at one location and moves toward a fully settled value. There is generally no obvious peak as in the kinetic energy transients, but rather an inflection point followed by a series of relatively small c.g. history maxima. This occurs as the liquid 1) accelerates as it moves aftward toward the sump, 2) decelerates following impact on the tank aft dome, and then 3) sloshes back and forth as the liquid motion damps. This behavior is typical of settling problems because the liquid generally starts in some location and moves toward an equilibrium position under applied thrust. Note that only the center-of-mass history in the direction of the net settling acceleration vector need be analyzed. The lateral c.g. will in general oscillate for a much longer time than required for engine start.

A third characterization of propellant settling is the size of the free-surface waves relative to the head over the tank drain. Once liquid reaches the aft section of the tank, propellant is theoretically available to the engine feed system. However, flow initiating in reduced-gravity environments before significant engine thrust buildup has the tendency to yield large vapor-ingestion heights where a column of gas is pulled through the liquid and ingested into the outlet. Gas ingestion in this manner is not to be confused with that due to vortexing, which serves to increase vapor-ingestion heights further. A measure to reduce the tendency for unplanned bubble ingestion is to ensure that the free-surface waves are smaller than the head over the outlet. A maximum wave-to-head ratio of approximately one-third is used in the present analysis, which is determined by eye from the three-dimensional free-surface plots. This criterion is confirmed for two natural periods of the tank–fluid system to verify that the slosh is damping.

Based on the preceding discussion, the following evaluation criteria are defined to determine when a propellant tank is adequately settled: First, all mean kinetic energy history maxima have occurred. Second, the propellant center-of-mass history in the direction of settling acceleration is asymptotic. Third, free-surface waves are less than one-third the head over outlet. In the present analysis, all three criteria are used to determine whether the propellant is adequately settled for main engine start as shown next for each simulated case.

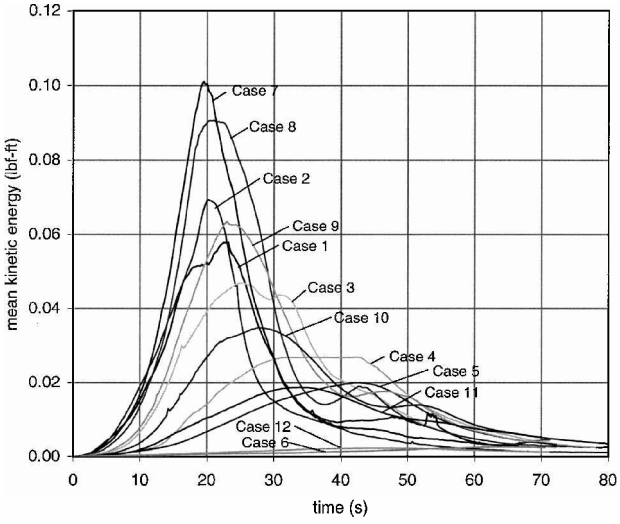

Fig. 5 Mean kinetic energy histories.

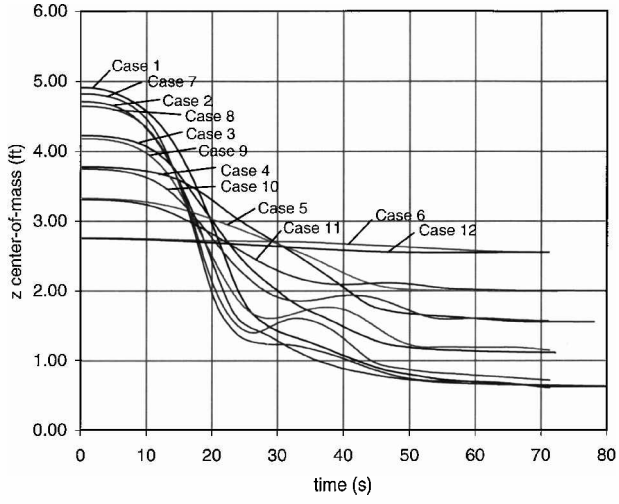

Fig. 6 Z center-of-mass histories.

Results

Propellant-settling performance for all cases is summarized in Figs. 5 and 6. Figure 5 shows the mean kinetic energy history in the liquid for each model executed. It is readily observed that propellant settling from an initially quiescent condition yields characteristic kinetic energy histories that are similar. Each simulation, thus, starts with zero kinetic energy, increases to some peak value, and then decreases back toward zero in an asymptotic fashion. In the present study, the $\theta = 20$ deg simulations (cases 7–12) exhibit higher peak kinetic energies and, thus, forces and moments than the $\theta = 0$ deg runs (cases 1–6) due to the additional damping from colliding slosh waves in the $\theta = 0$ deg cases. In cases 7–12, a more circular motion is witnessed, where the liquid traverses down one side of the tank and overshoots the outlet. However, a second pronounced kinetic energy peak due to splashing occurs after the first one, illustrating the longer propellant damping times for asymmetric initial liquid orientations in the tank.

The z center-of-mass histories in Fig. 6 show the asymptotic nature of the c.g. during settling. Here also, different characteristic curve shapes are noticed for the asymmetric and symmetric initial orientations. Because of the circular motion of propellant during settling in cases 7–12, a pronounced local peak in the center-of-mass history illustrates the overshoot of the outlet by the bulk propellant. Note that this variation is typically much more severe in unbaffled propellant tanks, which exhibit a series of geysers and the associated highly varying c.g. histories. The presence of slosh baffles in the tank, thus, significantly damps any postimpact slosh or geysering.

For most cases simulated, the first and second settling criteria are met after 60 s. However, the slosh wave magnitudes are still relatively large for several cases at this time. Refer to the free-surface histories in Figs. 7–18. Achievement of the third settling criterion is determined by direct observation of the graphical output of the simulations. It is observed that, for cases 6 and 12, which have large propellant volumes, adequate outlet coverage occurs after only 60 s of settling (Figs. 12 and 18). Conversely, scenarios with smaller fill fractions, such as cases 8 and 9, have significant slosh even after 70 s of settling (Figs. 14 and 15).

Although a constant burn time is simple, it unnecessarily wastes propellant during the large-fill-level scenarios. Accordingly, a linear relationship between settling time and fill fraction is recommended,

Fig. 7 Case 1 results; $f = 4\%$ and $\theta = 0$ deg.

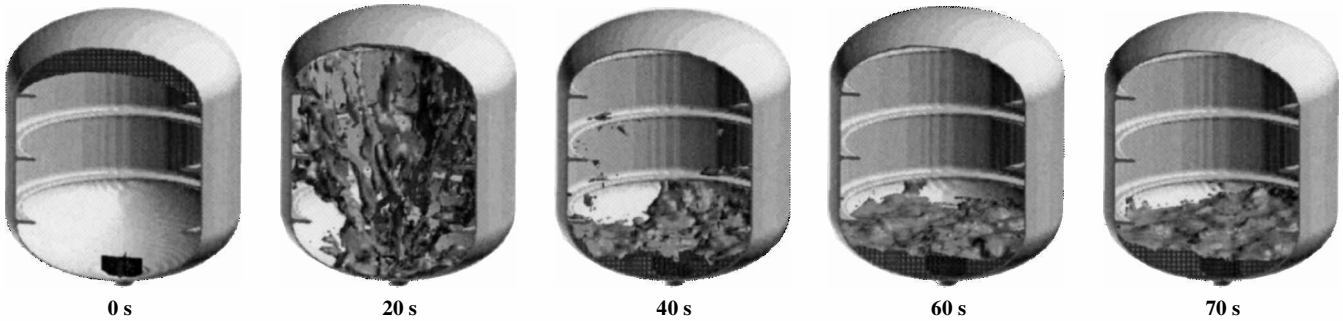

Fig. 8 Case 2 results; $f = 10\%$ and $\theta = 0$ deg.

a) 0 s b) 20 s c) 40 s d) 60 s e) 70 s

Fig. 9 Case 3 results; $f = 30\%$ and $\theta = 0$ deg.

a) 0 s b) 20 s c) 40 s d) 60 s e) 70 s

Fig. 10 Case 4 results; $f = 50\%$ and $\theta = 0$ deg.

a) 0 s b) 20 s c) 40 s d) 60 s e) 70 s

Fig. 11 Case 5 results; $f = 70\%$ and $\theta = 0$ deg.

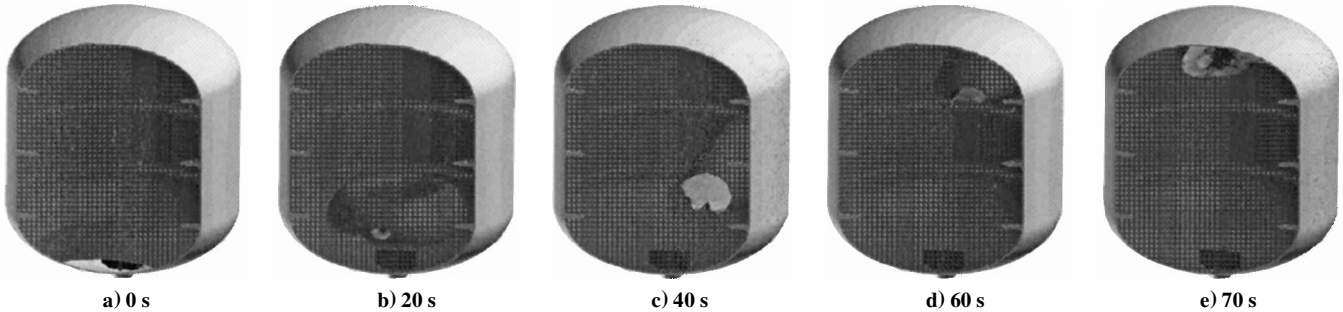

a) 0 s b) 20 s c) 40 s d) 60 s e) 70 s

Fig. 12 Case 6 results; $f = 95.5\%$ and $\theta = 0$ deg.

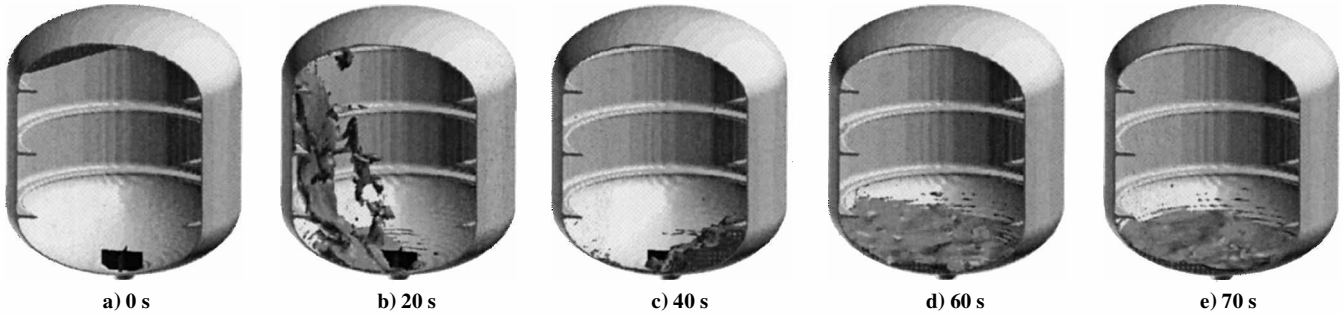

a) 0 s b) 20 s c) 40 s d) 60 s e) 70 s

Fig. 13 Case 7 results; $f = 4\%$ and $\theta = 20$ deg.

a) 0 s b) 20 s c) 40 s d) 60 s e) 80 s

Fig. 14 Case 8 results; $f = 10\%$ and $\theta = 20$ deg.

a) 0 s b) 20 s c) 40 s d) 60 s e) 80 s

Fig. 15 Case 9 results; $f = 30\%$ and $\theta = 20$ deg.

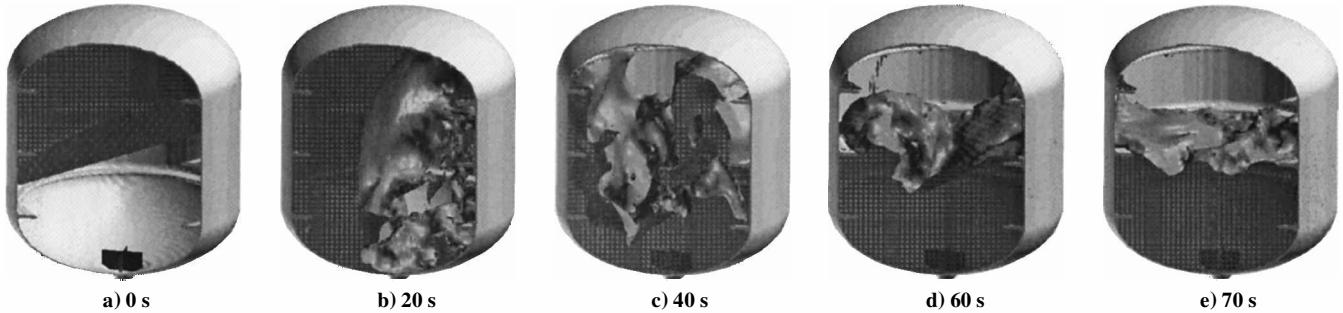

a) 0 s b) 20 s c) 40 s d) 60 s e) 70 s

Fig. 16 Case 10 results; $f = 50\%$ and $\theta = 20$ deg.

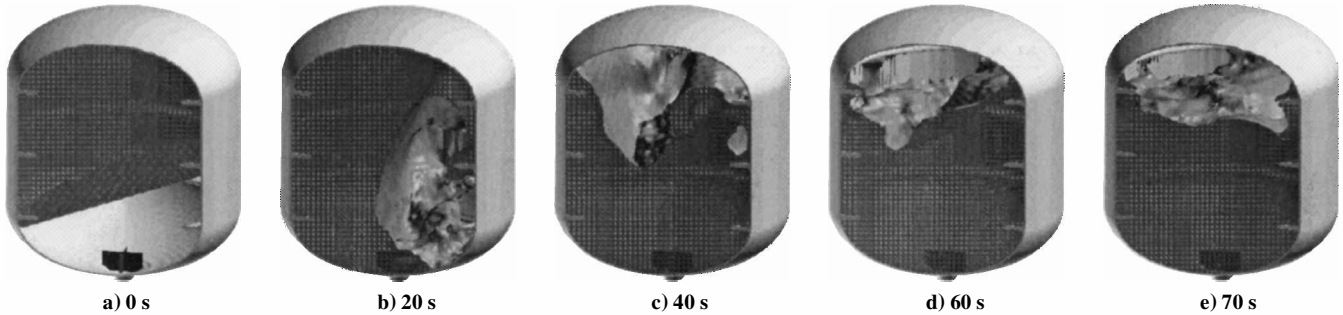

a) 0 s b) 20 s c) 40 s d) 60 s e) 70 s

Fig. 17 Case 11 results; $f = 70\%$ and $\theta = 20$ deg.

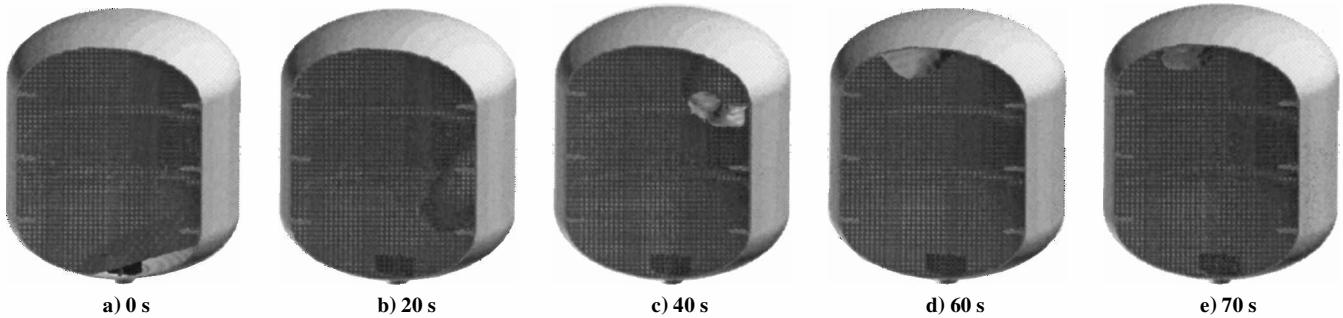

a) 0 s b) 20 s c) 40 s d) 60 s e) 70 s

Fig. 18 Case 12 results; $f = 95.5\%$ and $\theta = 20$ deg.

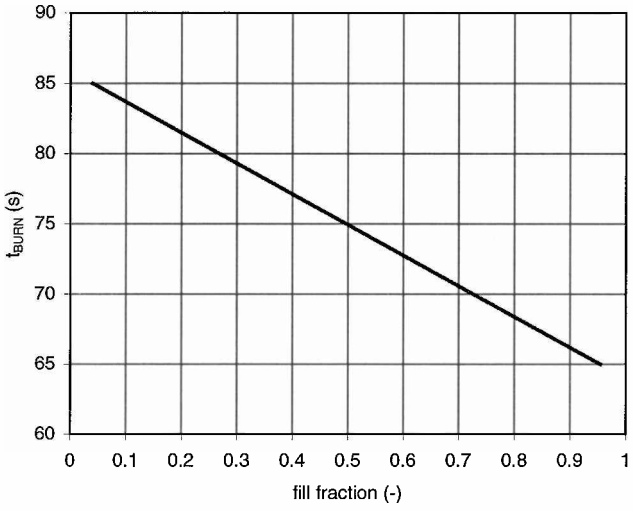

Fig. 19 Settling time vs fill fraction.

as shown in Fig. 19. Inclusive in the Fig. 19 plot is a 5-s performance margin; the relationship in equation form is

$$t_{\text{burn}} = -21.86f + 85.87 \tag{6}$$

for $0.040 < f < 0.955$, where t_{burn} is the thruster burn time (or settling time) and f is the fill fraction in the tank defined as the H_2O_2 volume divided by the empty tank volume. The 5-s margin in settling time adds design margin for the system to handle slosh environments slightly worse than those analyzed in the present study.

Conclusions

The numerical study described suggests that a variable thruster firing time between 65 and 85 s is adequate to settle the H_2O_2 propellant in the 4.6-ft-diam, 5.6-ft-long tank. This conclusion is based exclusively on computational fluid dynamics via the FLOW-3D software and several auxiliary models used to determine the appropriate inputs. Because of 1) code validation in surface-tension dominated environments, 2) code validation for slosh in large tanks, 3) a flight demonstrated CFD-based design methodology, and 4) a worst-case design approach, the present analysis is declared to be robust and conservative to ensure successful operation in orbit.

References

[1] *FLOW-3D User's Manual*, Flow Science, Inc., Los Alamos, NM, 1997.

[2] Bachelor, G. K., *Introduction to Fluid Dynamics*, Cambridge Univ. Press, New York, 1967, pp. 60–63.

[3] Der, J. J., and Stevens, C. L., "Liquid Propellant Tank Ullage Bubble Deformation and Breakup in Low-Gravity Reorientation," AIAA Paper 87-2021, June 1987.

[4] Patag, A. E., Hochstein, J. I., and Chato, D. J., "Modeling of Pulsed Propellant Reorientation," AIAA Paper 89-2727, July 1989.

[5] Sicilian, J. M., and Tegart, J. R., "Comparison of FLOW-3D Calculations with Very Large Amplitude Slosh Data," *Computational Experiments*, PVP-Vol. 176, American Society of Mechanical Engineers, Fairfield, NJ, 1989, pp. 23–30.

[6] Mikelis, N. E., Miller, J. K., and Taylor, K. V., "Sloshing in Partially Filled Liquid Tanks and Its Effect on Ship Motions: Numerical Simulations and Experimental Verification," Spring Meeting of the Royal Institution of Naval Architects, Paper 7, London, 1984.

[7] Grayson, G. D., and Cook, L. M., "Characteristics of the DC-XA Liquid Oxygen Propellant-Acquisition System," AIAA Paper 96-3081, July 1996.

[8] Fisher, M. F., Schmidt, G. R., and Martin, J. J., "Analysis of Cryogenic Behavior in Microgravity and Low Thrust Environments," AIAA Paper 91-2173, June 1991.

[9] Grayson, G. D., "Coupled Thermodynamic–Fluid-Dynamic Solution for a Liquid–Hydrogen Tank," *Journal of Spacecraft and Rockets*, Vol. 32, No. 5, 1995, pp. 918–921.

[10] Kolodzie, P. A., and Van Winkle, M., "Discharge Coefficients Through Perforated Plates," *AIChE Journal*, Vol. 3, No. 3, 1957.

[11] Smith, P. L., and Van Winkle, M., "Discharge Coefficients Through Perforated Plates at Reynolds Numbers of 400 to 3,000," *AIChE Journal*, Vol. 4, No. 3, 1958.

[12] Hochstein, J. I., Patag, A. E., and Chato, D. J., "Modeling of Impulsive Propellant Reorientation," AIAA Paper 89-0628, Jan. 1989.

[13] Navickas, J., and Madsen, R. A., "Propellant Behavior During Venting in an Orbiting Saturn S-IVB Stage," *Advanced Cryogenic Engineering*, Vol. 13, Plenum, New York, 1968, pp. 188–198.

[14] Hung, R. L., and Shyu, K. L., "Constant Reverse Thrust Activated Reorientation of Liquid Hydrogen with Geyser Initiation," *Journal of Spacecraft and Rockets*, Vol. 29, No. 2, 1992, pp. 279–285.

[15] Grayson, G. D., Watts, D. A., and Jurns, J. M., "Thermo-Fluid-Dynamic Modeling of a Contained Liquid in Variable Heating and Acceleration Environments," Fluids Engineering Div., American Society of Mechanical Engineers Summer Meeting, ASME Paper 3567, Vancouver, BC, Canada, June 1997.

J. A. Martin
Associate Editor